Cytochrome *c* Peroxidase−Cytochrome *c* Complex: Locating the Second Binding Domain on Cytochrome *c* Peroxidase with Site-Directed Mutagenesis†

Valerie W. Leesch,‡ Jordi Bujons,§ A. Grant Mauk,§ and Brian M. Hoffman*,‡

Department of Chemistry, Northwestern University, Evanston, Illinois 60208, and Department of Biochemistry and Molecular Biology, University of British Columbia, Vancouver, British Columbia V6T 1Z3, Canada

Received April 4, 2000

ABSTRACT: Cytochrome *c* peroxidase (C*c*P) can bind as many as two cytochrome *c* (C*c*) molecules in an electrostatic complex. The location of the two binding domains on C*c*P has been probed by photoinduced interprotein electron transfer (ET) between zinc-substituted horse cytochrome *c* (ZnC*c*) and C*c*P with surface charge-reversal mutations and by isothermal titration calorimetry (ITC). These results, which are the first experimental evidence for the location of domain 2, indicate that the weak-binding domain includes residues 146−150 on C*c*P. C*c*P(E290K) has a charge-reversal mutation in the tight-binding domain, which should weaken binding, and it weakens the 1:1 complex; K_1 decreases 20-fold at 18 mM ionic strength. We have employed two mutations to probe the proposed location for the weak-binding domain on the C*c*P surface: (*i*) D148K, a "detrimental" mutation with a net (+2) change in the charge of C*c*P, and (*ii*) K149E, a "beneficial" mutation with a net (−2) change in the charge. The interactions between Fe C*c* and C*c*P(WT and K149E) also have been studied with ITC. The C*c*P(D148K) mutation causes no substantial change in the 2:1 binding but an increase in the reactivity of the 2:1 complex. The latter can be interpreted as a long-range influence on the heme environment or, more likely, the enhancement of a minority subset of binding conformations with favorable pathways for ET. C*c*P(K149E) has a charge-reversal mutation in the weak-binding domain that produces a substantial increase in the 2:1 binding constant as measured by both quenching and ITC. For the 1:1 complex of C*c*P(WT), $\Delta G_1 = -8.2$ kcal/mol ($K_1 = 1.3 \times 10^6$ M^{-1}), $\Delta H_1 = +2.7$ kcal/mol, and $\Delta S_1 = +37$ cal/K·mol at 293 K; for the second binding stage, $K_2 < 5 \times 10^3$ M^{-1}, but accurate thermodynamic parameters were not obtained. For the 1:1 complex of C*c*P-(K149E), $\Delta G_1 = -8.5$ kcal/mol ($K_1 = 2 \times 10^6$ M^{-1}), $\Delta H_1 = +2.0$ kcal/mol, and $\Delta S_1 = +36$ cal/K·mol; for the second stage, $\Delta G_2 = -5.5$ kcal/mol ($K_1 = 1.3 \times 10^4$ M^{-1}), $\Delta H_2 = +2.9$ kcal/mol, and $\Delta S_2 = +29$ cal/K·mol.

Cytochrome *c* peroxidase (C*c*P)[1] catalyzes the two-electron reduction of hydrogen peroxide to water by ferrous cytochrome *c* (C*c*) (eq 1). In this process C*c*P reacts with H_2O_2

$$2Fe^{2+}Cc + H_2O_2 + 2H^+ \rightarrow 2Fe^{3+}Cc + 2H_2O \quad (1)$$

to form compound ES (*1*), which is a compound I that contains 1 oxidizing equivalent on the heme, in the form of an Fe^{4+}=O species, and one as a cation radical on tryptophan 191 (Trp 191) (*2, 3*). Compound *ES* then reacts sequentially with two molecules of Fe^{2+}C*c*, reduced first to compound II, in which either the heme or the Trp can be reduced, and finally back to the ferric resting state (eq 2). C*c*P is the only

$$Cc\text{P-I}(Fe^{4+}{=}O, Trp^{+\bullet}) \rightarrow [Cc\text{P} - \text{II}(Fe^{4+}{=}O) \leftrightharpoons Cc\text{P-II}(Trp^{+\bullet})] \rightarrow Cc\text{P}(Fe^{3+}) \quad (2)$$

peroxidase to obtain its reducing equivalents from a protein instead of a small molecule, and this fact combined with the early solution of the crystal structure at high resolution (*4*) has made it the prototypical system for the study of interprotein electron transfer (ET) (*5*−*7*). Nonetheless, the ET mechanism still is not understood in detail.

Interprotein ET between C*c*P and C*c* was originally assumed to occur through a tight-binding complex with 1:1 stoichiometry, such as was revealed in a key X-ray structure (*8*). However, although there has been disagreement (*8*−*10*), we have shown that C*c*P can bind C*c* at two distinct domains, one of which undoubtedly involves the surface area visualized in the crystal structure, and that a 2:1 complex can form over a range of ionic strengths (*11*−*13*). In our approach zinc is substituted for the iron in cytochrome *c*, allowing us to phototrigger the ET event, as shown in eq 3.

$$ZnCc, Fe^{3+}Cc\text{P} \xrightarrow{h\nu} {}^3(ZnP)Cc, Fe^{3+}Cc\text{P} \xrightarrow{k_{ET}} (ZnP)^{+\bullet}Cc, Fe^{2+}Cc\text{P} \quad (3)$$

The triplet excited state of ZnC*c* is quenched by Fe^{3+}C*c*P

† This work has been supported by NIH Grants HL13531 and HL 63203 (B.M.H.), MRC of Canada Grant MT-14021 (A.G.M.), and Ministerio de Educación y Ciencia of Spain postdoctoral fellowship (J.B.).

‡ Northwestern University.

§ University of British Columbia.

[1] Abbreviations: ET, electron transfer; C*c*P, cytochrome *c* peroxidase; C*c*, cytochrome *c*; ITC, isothermal titration calorimetry; K_i, association binding constant for the *i*th binding step; k_i, reactivity constant for the complex with *i* cytochrome *c* molecules bound.

10.1021/bi000760m CCC: $19.00
Published on Web 07/27/2000

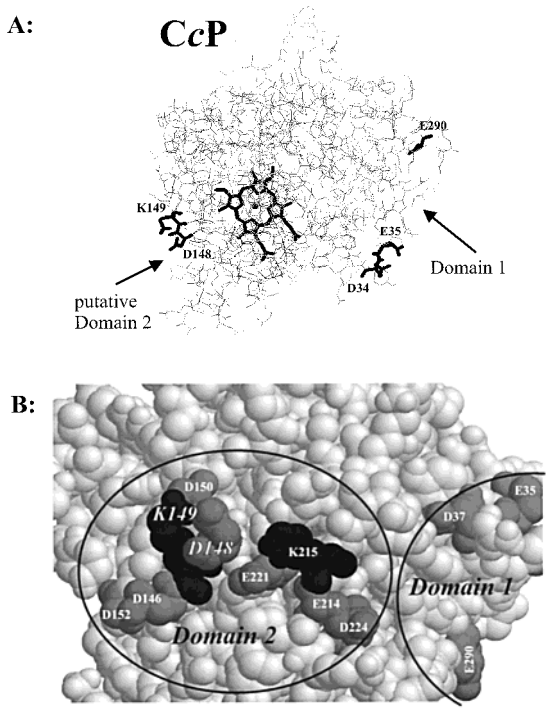

FIGURE 1: (A) Wire-frame diagram of cytochrome *c* peroxidase (C*c*P) with the heme shown in black. Locations of the two binding domains are indicated with arrows. (B) Space-filling model of C*c*P oriented to show domain 2. Charged residues are labeled; lysines are black, aspartates and glutamates are gray.

through a long-range electron-transfer process, transiently yielding ferrous C*c*P and the Zn-porphyrin cation radical, $(ZnP)^{+\bullet}$C*c*. Because the $Fe^{3+} \rightarrow Fe^{2+}$ heme reaction is being observed in C*c*P instead of the physiological $Fe^{4+}{=}O \rightarrow Fe^{3+}$ redox reaction, the tryptophan 191 cation radical is presumed not to be involved. Thus, necessarily, our experiment looks only at the direct heme−heme ET reaction, a simplification that eliminates complicating questions, such as whether the $Fe^{4+}{=}O$ or the $Trp^{+\bullet}$ is reduced first, and the role of internal ET between the two C*c*P redox centers (*14*−*17*).

The X-ray structure of the 1:1 complex, with C*c* bound at a location denoted domain 1, was interpreted as correlating the operative surface interactions between the two proteins with an electron-transfer pathway involving Trp191 (*8*), and some examinations of the physiological reaction kinetics have shown that the $Trp^{+\bullet}$ of compound *E*S is reduced first (*10*). Site-directed mutagenesis also has been important in identifying the negatively charged contact residues on C*c*P that are most crucial to binding to domain 1 (*18*, *19*). As to the second region that can bind C*c*, denoted domain 2, early Brownian dynamics simulations by Northrup et al. (*20*) suggested the possibility of binding near residue 148 of C*c*P, but no experimental evidence has addressed this question directly. As can be seen in Figure 1A, such a location for domain 2 would put it close to the C*c*P heme, and in fact we found that domain 2 is much more reactive for direct heme−heme ET between ZnC*c* and C*c*P than is domain 1, consistent with such a proposal (*21*).

We here report additional evidence about domain 1, and the first experimental evidence as to the location of domain 2, obtained through the study of three charge-reversal surface mutants of C*c*P, two of which are in the putative domain 2: (i) E290K, a glutamate → lysine mutant created to weaken the binding at domain 1 and at a residue that has been shown to be crucial to domain 1 binding in other mutagenesis studies (*18*); (ii) D148K, likewise created in order to *weaken* the binding to domain 2; and (iii) K149E, a lysine → glutamate mutation, in contrast, designed to *tighten* the binding to domain 2, as the positively charged lysine very near the proposed domain 2 could only be detrimental to binding a positively charged C*c*. We have used each of these C*c*P mutants as quenchers for ^{3}ZnC*c* in order to measure the effect of the surface mutations on the binding and reactivity at both domains. To complement the kinetics measurements, we have employed isothermal titration calorimetry (ITC) (*22*) as an independent measure of the binding for the C*c*P:C*c* complex, thereby revising the conclusions of earlier work by others (*9*).

EXPERIMENTAL PROCEDURES

Protein Preparation. Cytochrome *c* (type VI, horse heart) obtained from Sigma Chemical Co. was purified on a CM52 cation-exchange column (*23*) before use in calorimetry experiments. Zinc-substituted cytochrome *c* was prepared from horse heart cytochrome *c* according to published procedures (*24*, *25*). Recombinant cytochrome *c* peroxidase [C*c*P(MKT)] and the variants C*c*P(E290K), C*c*P(D148K), and C*c*P(K149E) were prepared and isolated as described elsewhere (*26*; J. Bujons, E. Lloyd, M. R. Mauk, and A. G. Mauk, manuscript in preparation). C*c*P(MKT) is a recombinant form that varies in sequence from the bakers' yeast C*c*P only at the N-terminus, where the residues MKT have been added. Previous constructs denoted as MKT have had errors in the sequence (D152G and T53I), which have been corrected in the C*c*P(MKT) and in all the variants studied here.

All potassium phosphate buffers were prepared with Milli-Q H_2O (resistivity ≥ 18 MΩ·cm). Fe^{3+}C*c* was exchanged into 10 mM phosphate buffer prior to use in calorimetry experiments. ZnC*c* was stored in 85 mM phosphate buffer and diluted into 10 mM phosphate just prior to use in quenching experiments. In most cases, C*c*P was stored as a crystalline suspension at 77 K and dissolved freshly on the day of the experiment. Deviation from this procedure, such as use of the same stock solution for several experiments, led to inconsistent results. Protein concentrations were determined optically on a Hewlett-Packard 8451A diode array spectrophotometer (Fe^{3+}C*c*, $\epsilon_{410} = 106$ mM^{-1} cm^{-1} or $\epsilon_{530} = 11$ mM^{-1} cm^{-1}; ZnC*c*, $\epsilon_{423} = 243$ mM^{-1} cm^{-1} or $\epsilon_{550} = 15.5$ mM^{-1} cm^{-1}; C*c*P, $\epsilon_{408} = 98$ mM^{-1} cm^{-1} or $\epsilon_{508} = 11.4$ mM^{-1} cm^{-1}).

Kinetic Measurements. All quenching measurements were carried out with samples of 18 mM ionic strength ($[KP_i] =$ 10 mM), pH 7.0. These samples were prepared in the dark; 2.0 mL of phosphate buffer containing an initial amount of ZnC*c* (2−20 μM) was purged slowly with nitrogen for 1.5−2 h. Stock solutions of C*c*P and ZnC*c* were also gently purged with nitrogen. Following verification of the intrinsic decay constant for ^{3}ZnC*c* at the initial concentration, reverse titrations were carried out by first adding a fixed amount of C*c*P (10−13 μM) followed by several increments of ZnC*c*. Typically only 3−6 data points for a titration were collected with one sample to minimize sample degradation.

The 532 nm output of a Nd−YAG pulsed laser (Continuum, YG660A) acted as the excitation source for ZnC*c*. A tunable polarizer (CVI Laser Corp.) reduced the incident power to 6 mJ/pulse to minimize degradation of the ZnC*c*. The sample was maintained at 20.0 ± 0.1 °C in a water-jacketed sample block. The decay of the triplet excited state of ZnC*c* (^{3}ZnC*c*) was monitored at 460 nm by transient absorption techniques; the probe light source (a 250 W tungsten halogen lamp) was passed through pre- and post-sample monochromators (Jobin Yvon). The data were collected with a LeCroy Model 9310 digitizer; the 50 000 raw data points obtained were logarithmically compressed to 3000 points for analysis. Typically between 2 and 5 progress curves were averaged, and sometimes a single shot was adequate; the signal-to-noise ratio was quite good and minimal averaging prevented degradation of the ZnC*c*. ^{3}ZnC*c* decays exponentially in the absence and presence of quencher (C*c*P), and these decays were fit to a single exponential to obtain the decay rate constant (k_{obs}).

Calorimetry Measurements. Isothermal titration calorimetry was carried out on a Microcal ITC titration calorimeter (Microcal, Inc.). The sample cell (volume = 1.34 mL) contained a 40−50 μM C*c*P solution; the reference cell contained distilled, deionized H_2O. A 1 mM FeC*c* solution was placed in the automated injection syringe and titrated in 20 injections of 10 or 12.5 μL. The syringe spun at a constant rate of 400 rpm to thoroughly mix the solutions and injections were made every 480 s. The temperature over the course of an experiment changed by less than 0.1 °C; the external temperature bath was maintained at 15 °C and the calorimeter thermostat at 20 °C. All experiments were carried out at 18 mM ionic strength ([KP_i] = 10 mM), pH 7.0. A control experiment, in which C*c* is titrated into 10 mM phosphate buffer, was performed in all cases to correct for the heat of dilution of the protein, which approaches zero over the course of the titration.

RESULTS

Quenching of ^{3}ZnCc by CcP(MKT). The photoinduced electron transfer (ET) between ^{3}ZnC*c* (horse) and recombinant cytochrome *c* peroxidase [C*c*P(MKT)] has been studied by measuring the quenching of ^{3}ZnC*c* as monitored at 460 nm. In the absence of quencher, ^{3}ZnC*c* decays exponentially with an intrinsic decay rate constant of $k_D = 67 \pm 3\ s^{-1}$, a rate that is independent of ZnC*c* concentration over the range studied. When quencher is present (Fe^{3+}C*c*P), the decay rate increases to a value denoted k_{obs}, but the traces remain exponential, indicative of rapid exchange (data not shown). Subtracting k_D from the observed decay rate constant (k_{obs}) gives the quenching rate constant Δk ($\Delta k = k_{obs} - k_D$). Reverse titrations, in which the probe (ZnC*c*) is titrated into the quencher (C*c*P) (*5*, *12*), were carried out at [C*c*P(MKT)] = 11.5 μM and [ZnC*c*] = 1−70 μM. The titration was fit to equations for a 2:1 binding model with rapid exchange (*5*), eq 4,

$$\Delta k = k_1\frac{[\text{ZnC}c\text{:C}c\text{P}]}{[\text{ZnC}c]_0} + k_2\frac{2[(\text{ZnC}c)_2\text{:C}c\text{P}]}{[\text{ZnC}c]_0} = k_1f_1 + k_2f_2 \quad (4)$$

where f_i (i = 1, 2) is the fraction of ZnC*c* bound and k_i is the reactivity constant of the 1:1 or 2:1 complex. In a reverse titration of Fe^{3+}C*c*P by ZnC*c* there is a nonzero value for the Δk intercept as [ZnC*c*] → 0, and this quantity, Δk_0, given by eq 5, was used to eliminate the 1:1 binding constant K_1 as a fitting parameter, as has been discussed in previous work (*12*):

$$\Delta k_0 = \frac{k_1K_1[\text{C}c\text{P}]_0}{1 + K_1[\text{C}c\text{P}]_0} \quad (5)$$

We have shown previously that reverse titrations of bakers' yeast C*c*P with ZnC*c* at low ionic strength give a characteristic "rise-and-fall" behavior (maximum in Δk for [ZnC*c*] ≠ 0) from which binding and reactivity constants for *both* the 1:1 and 2:1 complex can be obtained (*28*). The reverse quenching titration with recombinant C*c*P (Figure 2A) gives results comparable to those for bakers' yeast C*c*P (*12*). The association constant for the 1:1 complex, K_1, is the same within experimental error, 8.4 (8) × 10^5 M^{-1} for bakers' yeast C*c*P and 7.5 (4) × 10^5 M^{-1} for recombinant; K_2 did not change within the substantial experimental error, 4300 M^{-1} → 7000 M^{-1}; k_1 decreased slightly, from 38 s^{-1} to 27 s^{-1}; and k_2 decreased roughly 2-fold, from 770 s^{-1} to 380 s^{-1} (Table 1).

The parameters above describe the two thermodynamic binding steps, C*c*P + C*c* → C*c*P:C*c* and C*c*P:C*c* + C*c* → C*c*P:Cc_2. However, our goal is to obtain the microscopic binding and reactivity parameters for the individual binding domains, as defined in Scheme 1, which are related to the stoichiometric parameters by eqs 6−9:

$$K_1 = K_{10} + K_{20} \quad (6)$$

$$K_1K_2 = K_{10}K_{12} = K_{20}K_{21} \quad (7)$$

$$k_1 = {}^1k\frac{K_{10}}{K_1} + {}^2k\frac{K_{20}}{K_1} \quad (8)$$

$$k_2 = {}^1k + {}^2k \quad (9)$$

Of the four domain binding constants, only three are independent, thus the domain constants cannot be determined exactly (*29*). Nevertheless, it is possible to use these relationships to interpret the quenching titrations (see below).

Quenching of ^{3}ZnCc by CcP Variants. In the reverse titration with the mutant C*c*P(E290K), which contains an unfavorable charge-reversal mutation in the tight-binding domain, Δk decreases monotonically with the addition of the ZnC*c* photoprobe (Figure 2B). This means that, unlike the wild-type protein, the mutant shows only 1:1 overall binding. The titration was fit to eq 4a for 1:1 binding (*5*), giving K_1

$$\Delta k = k_1\frac{[\text{ZnC}c\text{:C}c\text{P}]}{[\text{ZnC}c]_0} = k_1f_1 \quad (4a)$$

= 3.8 × 10^4 M^{-1} and k_1 = 260 s^{-1} (Table 1); eq 5 for Δk_0 was used as a constraint as described above. The stoichiometric binding constant for the 1:1 complex, K_1, is reduced 20-fold by the replacement of glutamate 290 with an unfavorable positive charge; the second binding step has become too weak to observe under the experimental conditions.

Despite this loss of the second thermodynamic binding step, the reactivity constant, k_1, is increased 10-fold by the

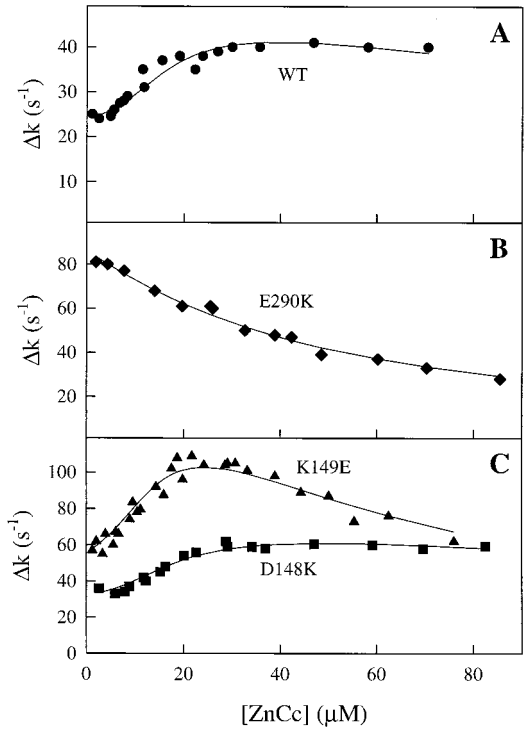

FIGURE 2: Reverse quenching titrations of C*c*P with ZnC*c*. (A) WT; [C*c*P(MKT)] = 11.5 μM. (B) Domain 1 mutation; [C*c*P-(E290K)] = 12.8 μM. (C) Domain 2 mutations; D148K (■) and K149E (▲). [C*c*P(D148K)] = 12.4 μM, [C*c*P(K149E)] = 10.5 μM. All experiments are at 18 mM ionic strength, pH 7.0, 20.0 °C.

Table 1: Binding and Reactivity Constants from ZnC*c*/C*c*P Quenching Titrations[a]

C*c*P variant	K_1 (M^{-1})	k_1 (s^{-1})	K_2 (M^{-1})	k_2 (s^{-1})
bakers' yeast	8.4(8) × 10^5	38 (4)	4 (1) × 10^3	7.7 (8) × 10^2
MKT	7.5 (4) × 10^5	26.6 (4)	7 (2) × 10^3	3.8 (8) × 10^2
E290K	3.8 (3) × 10^4	2.6 (2) × 10^2		
D148K	5.5 (2) × 10^5	36.6 (8)	5 (2) × 10^3	7 (2) × 10^2
K149E	1.0 (2) × 10^6	61 (2)	4.3 (6) × 10^4	3.3 (2) × 10^2

[a] Stoichiometric constants are obtained from fits of the reverse titrations to eqs 4 and 4a. Errors in the last digit of each constant are given in parentheses.

Scheme 1: Representation of Binding at Two Interacting Domains[a]

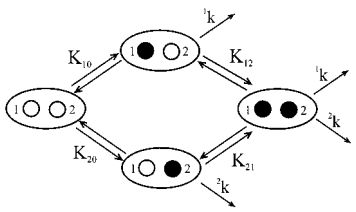

[a] C*c*P is an oval, the filled circles are occupied binding domains, and the unfilled circles are unoccupied binding domains.

mutation. This is easy to understand when one recalls that the first binding constant, K_1, reflects the formation of both types of 1:1 complexes, one with ZnC*c* bound at domain 1 and the other with ZnC*c* bound at domain 2 (eq 6). In the present case, the stoichiometric reactivity constant of the 1:1 complex, k_1, increases 10-fold because a larger proportion of the 1:1 complexes have ZnC*c* bound at the highly reactive, weakly binding domain. Specifically, by use of eqs 6−8 and with the assumption that K_{20} is approximately unchanged, the fraction of 1:1 complexes with C*c* bound in domain 2, given by the ratio K_{20}/K_1, increases from at least 0.01 for WT C*c*P to at least 0.2 for the mutant, and thus the high reactivity of domain 2 (large value of ^2k) contributes more significantly (eq 8).

Two charge-reversal mutations in a possible region for the weak-binding domain also have been studied: D148K, which would be expected to *weaken* the binding, and K149E, which would *tighten* the binding. The reverse titrations for both these mutants are shown in Figure 2C. The D148K titration demonstrates the shallow rise-and-fall behavior of the wild-type protein, while the K149E titration is considerably different: the quenching is greater, and the peak at [ZnC*c*]/[C*c*P] = 2 is much sharper. Stoichiometric binding and reactivity parameters were extracted from these titrations through the use of eqs 4 and 5.

For D148K, K_1 appears to be slightly less than for WT C*c*P [5.5 (2) × 10^5 M^{-1} vs 7.5 (4) × 10^5 M^{-1}, respectively (Table 1)]; the error in the value for K_2 is too large to tell with certainty if it is changed. The reactivity constant of the 1:1 complex is approximately 50% greater and that for the 2:1 complex is approximately 2-fold greater with D148K than with the WT protein.

For the K149E mutant, K_1 is little changed while the binding constant for the formation of the 2:1 complex, K_2, is 6-fold greater than it is with WT C*c*P, as anticipated. Further, the stoichiometric reactivity constant of the 1:1 complex is significantly higher (k_1 = 61 s^{-1}), reflecting the increased contribution of 1:1 binding at domain 2 to the reactivity. The reactivity constant of the 2:1 complex, k_2, is unchanged by the mutation within experimental error. This is expected if the mutation enhances the binding affinity of domain 2, K_{20}, without affecting the reactivity constants for either domain.

Titration Calorimetry. Figure 3A shows the incremental calorimetric titration of Fe^{3+}C*c* (horse) into Fe^{3+}C*c*P(MKT) at 10 mM phosphate, pH 7. In this experiment, $[CcP]_{initial}$ = 40 μM and C*c* is titrated to almost a 4:1 ratio. These data are corrected for the dilution of C*c* into 10 mM KP_i buffer. The error bars shown in the inset are based on the error in the raw peak area due to baseline noise.

The calorimetric titrations were fit by standard Marquardt methods (*30*) to two models provided in the software of the manufacturer (*22*). In a one-site model for the binding of C*c* by C*c*P, the total heat absorbed, Q, upon adding C*c*, total concentration $[Cc]_t$, to C*c*P at a total concentration $[CcP]_t$, is given by

$$Q = nV_0[CcP]_t F\Delta H \qquad (10)$$

where V_0 is the active solution cell volume, $n \approx 1$ is the number of binding sites, ΔH is the molar enthalpy of binding, and F is the fraction of $[CcP]_t$ with a C*c* bound:

$$F = \frac{K_1[Cc]_{free}}{1 + K_1[Cc]_{free}}$$

For an alternate model with two *independent* sites, denoted α and β, the heat, Q, is given by

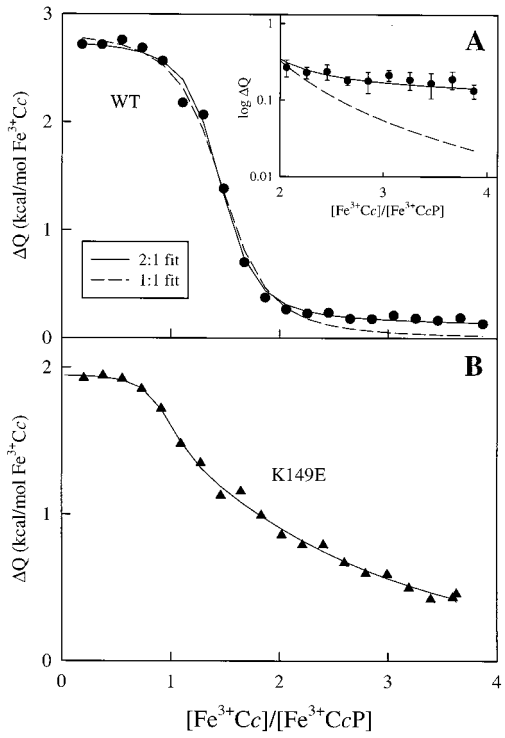

FIGURE 3: Incremental calorimetry titrations of C*c*P with Fe^{3+}C*c*. (A) WT; [C*c*P(MKT)] = 40 μM, 20.44 °C. Solid line is a 2:1 fit, dashed line is a 1:1 fit. (Inset) 2:1 fit (—), 1:1 fit (- - -), and error bars based on noise level of raw data are shown. (B) [C*c*P(K149E)] = 52 μM, 20.90 °C. Solid line is a 2:1 fit to the data. All experiments are at 18 mM ionic strength, pH 7.0.

$$Q = V_0[\mathrm{Cc P}]_t(n_\alpha F_\alpha \Delta H_\alpha + n_\beta F_\beta \Delta H_\beta) \qquad (11)$$

$$F_\alpha = \frac{\mathrm{K}_\alpha[\mathrm{Cc}]_{\mathrm{free}}}{1 + K_\alpha[\mathrm{Cc}]_{\mathrm{free}}} \qquad F_\beta = \frac{K_\beta[\mathrm{Cc}]_{\mathrm{free}}}{1 + K_\beta[\mathrm{Cc}]_{\mathrm{free}}} \qquad (12)$$

where $n = n_\alpha + n_\beta \approx 2$, $n_\alpha = n_\beta \approx 1$, and F_α and F_β are the fractional occupancies of the two sites. In both models, *n* values were allowed to float in the fitting and typically did not deviate more than 10−15% from unity. A calorimetric titration data set consists of differential heat changes, the changes in heat content from the completion of the $i - 1$ injection to the completion of the *i* injection, denoted $\Delta Q(i)$. As a result, it is the differentiated forms of eqs 10 and 11 with respect to [C*c*] that are relevant for comparison with experiment.

This two-site model nominally addresses the special case of independent binding at two noninteracting sites. However, the binding of two C*c* to C*c*P is likely to be correlated because electrostatics play a large role in complexation. Fortunately, the model also can describe a system with interacting sites. To do so, the two binding parameters that are generated by eqs 11 and 12 (K_α and K_β) are treated as "ghost-site" binding constants (*31*). Such ghost parameters, which have no physical relevance, are combinations of the physically meaningful parameters for the two physical sites given by eq 13. This analysis allows for cooperativity and

$$K_1 = K_\alpha + K_\beta \qquad K_1K_2 = K_\alpha K_\beta \qquad (13)$$

site−site interaction. In the case where the binding at one site is much tighter than the other, this procedure gives real (not imaginary or complex) stoichiometric constants for the unconstrained 2:1 model (eq 4). Similarly, the enthalpies of eq 11 are "ghost-site" enthalpies; the unconstrained stoichiometric enthalpies for the first and second binding steps (ΔH_1 and ΔH_2) can be calculated by

$$\Delta H_1 = \Delta H_\alpha \frac{K_\alpha}{K_1} + \Delta H_\beta \frac{K_\beta}{K_1} \qquad \Delta H_2 = \Delta H_\alpha \frac{K_\beta}{K_1} + \Delta H_\beta \frac{K_\alpha}{K_1} \qquad (14)$$

Table 2: Binding and Thermodynamic Constants Obtained from FeC*c*/C*c*P Titration Calorimetry[a]

C*c*P variant	MKT	K149E
K_1 (M^{-1})	1.3 (6) × 10^6	2 (1) × 10^6
ΔG_1 (kcal/mol)	−8.2 (3)	−8.5 (3)
ΔH_1 (kcal/mol)	+2.7 (3)	+2.0 (2)
ΔS_1 (cal/K·mol)	+37 (2)	+36 (2)
K_2 (M^{-1})	< 5 × 10^3	1.3 (3) × 10^4
ΔG_2 (kcal/mol)	> −5	−5.5 (1)
ΔH_2 (kcal/mol)		+2.9 (6)
ΔS_2 (cal/K·mol)		+29 (2)

[a] Constants are obtained from a fit to eq 11 followed by conversion to stoichiometric constants with eqs 13 and 14. Errors in the last digit of each constant are given in parentheses.

The fit to the 2:1 binding model (eq 11) is shown as a solid line through the data in Figure 3A, and the fit to a 1:1 binding model (eq 10) is shown as a dashed line. The 2:1 model clearly provides a better fit to the data in the region where binding of the second C*c* would contribute, namely, where C*c* is in excess over C*c*P (Figure 3A, inset). The intrinsic parameters for the first binding step are determined with reasonable precision [$K_1 = 1.3\ (6) \times 10^6\ M^{-1}$ and $\Delta H_1 = 2.7$ (3) kcal/mol; Table 2] and agree well both with the quenching measurements described above and with previous calorimetry experiments by Erman and co-workers (*9*), who found $K_1 = 1.5\ (5) \times 10^6\ M^{-1}$ and $\Delta H_1 = 2.05$ (5) kcal/mol at pH 6 and 20 mM ionic strength. The binding constant and enthalpy were used to calculate the free energy and entropy for the first binding step: $\Delta G_1 = -8.2$ (3) kcal/mol and $\Delta S_1 = +37$ (2) cal/K·mol at 293.6 K. Thus, the first binding step, with C*c* bound primarily at the tight binding domain, is dominated by a large favorable entropy. Because the second binding step is quite weak and the concentrations of the proteins are relatively low, the 2:1 fit does not give independently reliable values for K_2 and ΔH_2; the statistical correlation between these parameters is close to unity, and thus many combinations of these parameters give good fits to the data. Only an upper bound of $K_2 \leq 5 \times 10^3\ M^{-1}$ can be placed on the binding parameter; ΔH_2 is positive but is not well determined.

Figure 3B shows the calorimetric titration of Fe^{3+}C*c* (horse) into the mutant Fe^{3+}C*c*P(K149E) at 10 mM phosphate, pH 7. In this experiment, $[\mathrm{K149E}]_{\mathrm{initial}} = 52\ \mu$M, and C*c* is added up to a 3.5:1 ratio. As with the WT protein, the data has been corrected for the titration of C*c* into buffer. The titration with this mutant again reflects 2:1 binding (Figure 3A), and for both WT and K149E C*c*P, the regions where [C*c*]/[C*c*P] < 1 are similar, showing areas of saturation indicating a tight 1:1 complex. However, at higher ratios the titration with the K149E mutant is quantitatively different from the titration with WT C*c*P: the shallow decline in ΔQ for [C*c*]/[C*c*P(K149E)] > 1 reflects a far larger contribution to the evolved heat from the 2:1 complex than for the WT C*c*P.

A 1:1 binding model is completely unable to describe the K149E data. Table 2 contains the parameters obtained from the fit to the 2:1 binding model described in eq 11 after conversion from ghost constants to stoichiometric constants. The calorimetric K_1 agrees within experimental error with that measured by excited-state quenching. The value $K_2 = 1.3\ (2) \times 10^4\ M^{-1}$ is significantly greater than that measured for WT by either quenching or calorimetry; thus, replacement of the lysine residue 149 by a glutamate tightens the binding of C*c* to domain 2 and thereby stabilizes the 2:1 complex. The binding enthalpies measured for the K149E mutant are $\Delta H_1 = 2.0$ (2) kcal/mol and $\Delta H_2 = 2.9$ (6) kcal/mol, which lead to the following free energies and entropies of binding: $\Delta G_1 = -8.5$ (3) kcal/mol and $\Delta S_1 = +36$ (2) cal/K·mol for the first binding step, and $\Delta G_1 = -5.5$ (1) kcal/mol and $\Delta S_1 = +29$ (2) cal/K·mol for the second step. Again, both binding steps are dominated by positive entropy changes.

DISCUSSION

We have examined the binding of cytochrome *c* to C*c*P by measuring quenching of ^{3}ZnC*c* by C*c*P(MKT) and directly by isothermal calorimetry. Previous studies of C*c*P in our lab used C*c*P isolated from bakers' yeast. Here we used the recombinant protein C*c*P(MKT) in which the sequence errors D152G and T53I present in an earlier cloned C*c*P have been corrected (*26*). We note that residue 152 is near the proposed location of the weak binding domain (Figure 1) and that the replacement of the aspartate with a glycine could be detrimental to either binding or ET reactivity; future work will attempt to address this issue. Thus, it is perhaps significant that these sequence errors are present in the versions of C*c*P used by many researchers in the last several years, in particular in work that challenged the significance of the 2:1 complex (*10*). Clearly, one should be cautious when comparing data from authentic and recombinant proteins when there are *known* sequence errors in the recombinant protein.

The published reverse titration between ZnC*c* (horse) and bakers' yeast C*c*P at 10 mM phosphate, pH 7 (*12*), has been repeated here for the recombinant C*c*P(MKT) (Figure 2A) and the results are very similar. Both the binding constant for the 1:1 complex (K_1) and that for the 2:1 complex (K_2) are essentially unchanged within experimental error. The reactivity constants of both types of complex are slightly decreased for recombinant C*c*P over authentic C*c*P; k_2 is decreased by approximately 2-fold. However, the reactivity constant of the 2:1 complex (k_2) is still at least 10 times greater than the reactivity constant of the 1:1 complex (k_1). The results show that for our experiments the bakers' yeast and MKT C*c*P are experimentally interchangeable, though not completely indistinguishable.

The complex between C*c*P(MKT) and Fe^{3+}C*c* also was studied by titration calorimetry. As shown in Figure 3A, the 2:1 model fits the calorimetric data in the region where C*c* is in excess, as can be seen best in the inset to Figure 3A, with $K_1 = 1.3\ (6) \times 10^6\ M^{-1}$ and $K_2 \leq 5 \times 10^3\ M^{-1}$. K_1 and the upper bound for K_2 obtained from ITC at pH 7 agree well with the results from the quenching measurements described above. Both binding steps are enthalpically unfavorable ($\Delta H_1 = +2.7$ kcal, $\Delta H_2 > 0$), and are dominated by favorable entropy changes ($\Delta S_1 = +37$ cal/K·mol). It is important to note that 1:1 binding with a binding constant on the order of $10^5-10^6\ M^{-1}$ *cannot* give a measurable amount of heat in the portion of a titration where C*c* is in excess. Since the heat released in this region indeed is significantly different from zero outside of all possible experimental error, the measurement unambiguously confirms the formation of a 2:1 complex at pH 7. In previous studies, Erman and co-workers (*9*) were unable to detect the presence of the 2:1 complex at pH 6. This likely is not a disagreement, because previous work in our laboratory showed that C*c*P and C*c* bind more weakly at lower pH (*11*). More recent ITC measurements by Wang and Pielak (*32*) have shown 1:1 binding in the physiological yeast C*c*−yeast C*c*P complex, but they state that a $K_2 \leq 10^4\ M^{-1}$ would be undetectable in their experiment, and thus their results and ours are compatible.

The titration calorimetry experiments do not determine K_2 with precision because the maximum product of the concentration of C*c*P (40 μM) and the approximate binding constant ($5 \times 10^3\ M^{-1}$) is only K_1[C*c*P] ~ 0.2, which is not high enough to produce enough 2:1 complex to measure K_2 accurately. Indeed, one of the reasons that weak binding has been difficult to detect is that many experiments, including many of our own, are carried out at concentrations of 5−10 μM, to make optical measurements easy. Current work in our lab involving the myoglobin−cytochrome b_5 complex has detected weak binding definitively at millimolar concentrations (M. Jiang, Q. Ning, and B. M. Hoffman, manuscript in preparation), and calorimetry studies at higher concentration ([C*c*P] $\approx$ 0.5 mM) will be reported in due course.

Domain 1 Mutation, E290K. Many studies have been performed with mutations in the tight-binding domain, and its location has been well mapped by a number of techniques (*18, 34*). In particular, the charge-neutralization mutant E290N studied by Miller and co-workers (*35*) was one of the mutations that was most detrimental to domain 1 binding, as measured by both steady-state kinetics and calorimetry. In the present work, we have examined the charge-reversal mutant E290K, which has a net unfavorable charge change of +2. This mutation causes a 20-fold decrease in K_1 and abolishes detectable 2:1 binding (Figure 2B). Recall that 2:1 binding is dependent on the binding at *both* domains, and thus, as observed for C*c*P(D37K) (*19*), when the binding for both domains 1 and 2 is weak, not enough 2:1 complex forms in this concentration range to be observable. The *apparently* anomalous effect of the 1:1 complex reactivity increasing 10-fold occurs because a larger percentage of C*c*P molecules have C*c* bound at the more-reactive domain 2 (eq 8, Scheme 1).

It is interesting that this single charge-reversal mutation in domain 1 has such a large detrimental effect on the binding, because the Brownian dynamics simulations of Northrup et al. (*20*) show many possible conformations of the complex in the domain 1 region, and thus one might have expected that the charge reversal at position 290 would simply cause the C*c* to reposition itself, binding in an alternate geometry involving other negative residues in the domain. We infer that the E290−K73 salt bridge between C*c*P and C*c* indicated in the crystal structure (*8*) is crucial to achieving the proper complex orientation for ET and thus precludes this option.

Domain 2 Mutations, D148K and K149E. The Brownian dynamics simulations by Northrup et al. (*20*) also showed several potential docking locations for C*c* on the side of C*c*P opposite from the well-established domain 1, in the vicinity of Asp 148. We have employed two mutations to probe this region of the C*c*P surface: (i) D148K, a "detrimental" mutation with a net (+2) change in the charge of C*c*P, and (ii) K149E, a "beneficial" mutation with a net (−2) change in the charge (Figure 1).

The binding constant for the 1:1 complex of C*c* with C*c*P-(D148K) is slightly reduced, but even with the large errors (Table 1), it is clear that the D148K mutation does not have the drastic effect on domain 2 binding that E290K has on domain 1. Thus, the *binding* result does not support the hypothesis that D148 forms part of the second domain. On the other hand, recall that the reactivity constant of the 2:1 complex is actually twice as high for the D148K vs WT C*c*P, so the mutation is not without a significant effect. Bujons et al. (manuscript in preparation) have shown using ^{1}H NMR that several heme resonances are perturbed in the D148K mutant. This long-range influence on the heme environment could account for the increase in heme−heme ET rate. Alternatively, the loss of the negative contact with D148 might enhance a minority subset of binding conformations with favorable pathways for ET, without a substantial change in affinity (*36*). Figure 1B shows that there are several other negative residues in the vicinity of the putative domain 2 that may be more crucial to binding, such as residues 221 and 224, which were shown in surface modification experiments by Bechtold and Bosshard (*37*) to be involved in binding.

The K149E mutant was constructed in an attempt to tighten the binding in domain 2. Lysine 149 sits in the middle of several negative residues in the proposed domain 2 location, and its presence can only hamper binding by C*c* (Figure 1). This mutation has a strong effect on the titration with ZnC*c* (Figure 2C): K_2 increases 6-fold over WT C*c*P, while k_1 increases more than 2-fold. The increase in K_2 reflects the increase in the weak-site binding constant (see below). Just as with the E290K mutant, the increase in k_1 is caused by a change in the relative reaction contribution in a 1:1 complex with ZnC*c* at domain 1 vs domain 2 (the partition between ^1k and ^2k), but in this case the contribution from domain 2 increases because K_{20} (domain 2 binding constant) is increased by the mutation, rather than because K_{10} (domain 1 binding constant) is decreased (eq 8). The reactivity constant k_2, which is simply a sum of the reactivity constants of the two domains, is unchanged (eq 9). This fact suggests that we have in fact enhanced the binding at an already existing domain as opposed to creating a new binding domain. The results for this mutant clearly support the hypothesis that domain 2 is located in the proposed region shown in Figure 1. This conclusion is corroborated by the potentiometric titration results of Bujons et al. (manuscript in preparation). Using yeast C*c* instead of horse, they saw not only tighter 2:1 binding with K149E but also weaker 2:1 binding with D148K.

The quenching measurements are supported by titration calorimetry. Both techniques (i) show 2:1 binding for WT and K149E C*c*P and (ii) show that the K149E mutation enhances binding to domain 2 significantly. Although the value for K_2 measured by calorimetry (1.3×10^4 M^{-1}) is smaller than that measured by quenching titration (4.3×10^4 M^{-1}), binding is substantially increased in either experiment. Enthalpies for both binding steps were obtained for the K149E mutant. The enthalpies for both binding steps are unfavorable ($\Delta H > 0$), with that for the second binding step, $\Delta H_2 = 2.9$ kcal/mol, being more unfavorable than that for the first, $\Delta H_1 = 2.0$ kcal/mol. As with WT C*c*P, binding to C*c*P(K149E) in both domains is dominated by a favorable entropy term. This is typical for protein−protein interactions and is explained by the expulsion of water molecules from the surfaces of the proteins during binding, which increases the entropy (*31*, *38*).

Table 3: C*c*P(MKT) Domain Constants at Two Limits[a]

domain constant	zero cooperativity limit	E290K limit
K_{10} (M^{-1})	7.4×10^5	7.2×10^5
K_{20} (M^{-1})	7×10^3	2.7×10^4
K_{21} (M^{-1})	7.4×10^5	1.9×10^5
K_{12} (M^{-1})	7×10^3	7.3×10^3
^1k (s^{-1})	23.5	14
^2k (s^{-1})	360	370
ΔG_{coop} (kcal/mol)	0	+0.80

[a] Domain constants are calculated from stoichiometric constants by use of eqs 6−9.

Domain Parameters for CcP(MKT). The measured stoichiometric binding and reactivity constants for C*c*P and C*c* can be used to set limits on the six domain constants (eqs 6−9, Scheme 1) (*29*, *39*, *40*), and these limits are narrowed by a few reasonable assumptions. First, we assume that at low ionic strength it is harder to bind a second molecule of C*c* when a first molecule is already bound ($K_{10} \geq K_{21}$ and $K_{20} \geq K_{12}$). This is reasonable given that at low ionic strength, where shielding by solvent ions is minimal, there will be some repulsive interaction between two C*c* molecules. Second, we assume that a mutation in one domain will have no measurable direct effect on the binding and reactivity in the other domain, which is on the opposite side of the protein. For example, we can assume that the E290K mutation in domain 1 does not change parameters for domain 2, K_{20} and ^2k (Scheme 1). We do not need to assume the same for the domain 2 mutations because the resulting limits on the domain parameters correspond to positive cooperativity, which is eliminated by the first assumption.

The permitted values for domain constants, which cannot be known exactly, were determined from the stoichiometric binding and reactivity constants from quenching measurements (Table 1), as constrained by the above assumptions, and are given in Table 3. For WT C*c*P, the reactivity constant of domain 1 is low ($^1k = 14-24$ s^{-1}), while that of domain 2 is over 10-fold higher ($^2k = 360-370$ s^{-1}). The binding constant for a C*c* at domain 1, but with domain 2 empty, is $K_{10} = (7.2-7.4) \times 10^5$ M^{-1}, while with a C*c* already bound at domain 2 it could be as low as $K_{21} = 1.9 \times 10^5$ M^{-1}. Similarly, the binding constant for domain 2 with domain 1 empty is $K_{20} = (1-3) \times 10^4$ M^{-1}, while with a C*c* already bound at domain 1 it can be no greater than 0.7×10^4 M^{-1}. From the range of domain binding constants, we can place limits on the ΔG of binding cooperativity, ΔG_{coop}. Thus, assuming binding cooperativity is negative, the free energy penalty paid for binding a second C*c* when one is bound already can be no more than +0.8 kcal/mol.

SUMMARY

We have shown in this work that (i) the binding of C*c* and ET reactivity of recombinant C*c*P(MKT) are similar to those of bakers' yeast C*c*P in the reaction with ZnC*c*; (ii) 2:1 binding is detected for WT C*c*P both by ET measurements and by titration calorimetry, which is independent of the measure of reactivity; (iii) the "unfavorable" C*c*P charge-reversal mutation E290K drastically weakens the binding to domain 1, consistent with previous findings; (iv) the D148K mutation has little, if any, effect on domain 2 binding but increases reactivity; (v) the K149E mutation tightens the binding to domain 2, providing the first direct identification of a residue near the weak binding domain; and (vi) the rate constant for reactivity in the 2:1 complex (k_2) is unchanged in the K149E mutant, although the binding is tighter, which indicates that the location and orientation of C*c* on the domain 2 surface is similar. Thus, domain 2 comprises a region that includes residue 149, in the region where the heme of C*c*P is closest to the surface of the protein.

ACKNOWLEDGMENT

We thank the Keck Biophysics Facility at Northwestern University for the use of the isothermal titration calorimeter [http://x.biochem.northwestern.edu/Keck/keckmain.html].

REFERENCES

1. Yonetani, T. (1976) in *The Enzymes, Vol XIII* (Boyer, P. D., Ed.) pp 345−361, Academic Press, Orlando, FL.
2. Sivaraja, M., Goodin, D. B., Smith, M., and Hoffman, B. M. (1989) *Science 245*, 738−740.
3. Huyett, J. E., Doan, P. E., Gurbiel, R., Houseman, A. L. P., Sivaraja, M., Goodin, D. B., and Hoffman, B. M. (1995) *J. Am. Chem. Soc. 117*, 9033−9041.
4. Finzel, B. C., Poulos, T. L., and Kraut, J. (1984) *J. Biol. Chem. 259*, 13027−13036.
5. Nocek, J. M., Zhou, J. S., De Forest, S., Priyadarshy, S., Beratan, D. N., Onuchic, J. N., and Hoffman, B. M. (1996) *Chem. Rev. 96*, 2459−2489.
6. McLendon, G., and Hake, R. (1992) *Chem. Rev. 92*, 481−490.
7. Millett, F., Miller, M. A., Geren, L., and Durham, B. (1995) *J. Bioenerg. Biomembr. 27*, 341−351.
8. Pelletier, H., and Kraut, J. (1992) *Science 258*, 1748−1755.
9. Kresheck, G. C., Vitello, L. B., and Erman, J. E. (1995) *Biochemistry 34*, 8395−8405.
10. Miller, M. A., Geren, L., Han, G. W., Saunders, A., Beasley, J., Pielak, G. J., Durham, B., Millett, F., and Kraut, J. (1996) *Biochemistry 35*, 667−673.
11. Stemp, E. D. A., and Hoffman, B. M. (1993) *Biochemistry 32*, 10848−10865.
12. Zhou, J. S., and Hoffman, B. M. (1994) *Science 265*, 1693−1696.
13. Mauk, M. R., Ferrer, J. C., and Mauk, A. G. (1994) *Biochemistry 33*, 12609−12614.
14. Ho, P. S., Hoffman, B. M., Kang, C. H., and Margoliash, E. (1983) *J. Biol. Chem. 258*, 4356−4363.
15. Hazzard, J. T., and Tollin, G. (1991) *J. Am. Chem. Soc. 113*, 8956−8957.
16. Matthis, A. L., Vitello, L. B., and Erman, J. E. (1995) *Biochemistry 34*, 9991−9999.
17. Miller, M. A. (1996) *Biochemistry 35*, 15791−15799.
18. Miller, M. A., Liu, R., Hahm, S., Geren, L., Hibdon, S., Kraut, J., Durham, B., and Millett, F. (1994) *Biochemistry 33*, 8686−8693.
19. Zhou, J. S., Tran, S. T., McLendon, G., and Hoffman, B. M. (1997) *J. Am. Chem. Soc. 119*, 269−277.
20. Northrup, S. H., Boles, J. O., and Reynolds, J. C. L. (1988) *Science 241*, 67−70.
21. Zhou, J. S., Nocek, J. M., DeVan, M. L., and Hoffman, B. M. (1995) *Science 269*, 204−207.
22. Wiseman, T., Williston, S., Brandts, J. F., and Lin, L. N. (1989) *Anal. Biochem. 179*, 131−137.
23. Brautigan, D. L., Ferguson-Miller, S., and Margolish, E. (1978) *Methods Enzymol. 53*, 128−164.
24. Vanderkooi, J. M., Adar, F., and Erecinska, M. (1976) *Eur. J. Biochem. 64*, 381−387.
25. Zhou, J. S., and Kostic, N. M. (1993) *J. Am. Chem. Soc. 115*, 10796−10804.
26. Ferrer, J. C., Turano, P., Banci, L., Bertini, I., Morris, I. K., Smith, K. M., Smith, M., and Mauk, A. G. (1994) *Biochemistry 33*, 7819−7829.
27. Deleted in press.
28. Zhou, J. S., and Hoffman, B. M. (1993) *J. Am. Chem. Soc. 115*, 11008−11009.
29. Klotz, I. M. (1986) *Introduction to Biomolecular Energetics, Including Ligand−Receptor Interactions*, Academic Press, Orlando, FL.
30. Marquardt, D. W. (1963) *J. Soc. Ind. Appl. Math. 11*, 431−441.
31. Klotz, I. M. (1997) *Ligand−receptor energetics: a guide for the perplexed*, Wiley, New York.
32. Wang, X., and Pielak, G. J. (1999) *Biochemistry 38*, 16876−16881.
33. Deleted in press.
34. Corin, A. F., Hake, R. A., McLendon, G., Hazzard, J. T., and Tollin, G. (1993) *Biochemistry 32*, 2756−2762.
35. Erman, J. E., Krescheck, G. C., Vitello, L. B., and Miller, M. A. (1997) *Biochemistry 36*, 4054−4060.
36. Liang, Z.-X., Nocek, J. M., Kurnikov, I. V., Beratan, D. N., and Hoffman, B. M. (2000) *J. Am. Chem. Soc. 122*, 3552−3553.
37. Bechtold, R., and Bosshard, H. R. (1985) *J. Biol. Chem. 260*, 5191−5200.
38. Dunitz, J. D. (1994) *Science 264*, 670.
39. Nocek, J. M., Zhou, J. S., and Hoffman, B. M. (1997) *J. Electroanal. Chem. 438*, 55−60.
40. Nocek, J. M., Leesch, V. W., Zhou, J. S., Jiang, M., and Hoffman, B. M. (2000) *Isr. J. Chem. 40* (in press).

BI000760M